BIOCHEMISTRY
including biophysical chemistry & molecular biology
Article

Biochemistry **2010,** *49,* 287–296 287
DOI: 10.1021/bi9017895

Synthetic Fusion Peptides of Tick-Borne Encephalitis Virus as Models for Membrane Fusion†

Jinhe Pan, C. Benjamin Lai, Walter R. P. Scott, and Suzana K. Straus*

Department of Chemistry, University of British Columbia, 2036 Main Mall, Vancouver, British Columbia V6T 1Z1, Canada

Received October 17, 2009; Revised Manuscript Received December 8, 2009

ABSTRACT: The fusion peptide of TBEV is a short segment of the envelope protein that mediates viral and host cell membrane fusion at acidic pH. Previous studies on the E protein have shown that mutations at L107 have an effect on fusogenic activity. Structural studies have also suggested that during the fusion process the E protein rearranges to form a trimer. In the present study, a number of short peptides were synthesized, and their structure/activity was examined: (1) monomers consisting of residues 93−113 of the wild-type E protein with Leu at position 107 (WT) and two mutants, namely, L107F and L107T; (2) a monomer consisting of residues 93−113 of the E protein with a C105A mutation (TFPmn); (3) a trimer consisting of three monomers described in (2), linked at the C-terminus via 1 Lys (TFPtr); (4) a monomer consisting of residues 93−113 of the E protein plus six additional Lys at the C-terminus; and (5) a trimer consisting of three monomers described in (3), linked via the side chain of the sixth lysine. The secondary structure content of all peptides was investigated using circular dichroism (CD). Approximately seven of the residues were in β-strand conformation, in the presence of POPC/POPE/cholesterol. The structures did not depend on pH significantly. The fusogenicity of the peptides was measured by FRET and photon correlation spectroscopy. The data suggest that TFPtr is the most fusogenic at acidic pH and that the mutation from L107 to T reduces activity. Molecular dynamics simulations of WT, L107T, and L107F suggest that this reduction in activity may be related to the fact that the mutations disrupt trimer stability. Finally, tryptophan fluorescence experiments were used to localize the peptides in the membrane. It was found that WT, L107F, TFPmn, and TFPtr could penetrate better into the acyl chain region of the lipids than the other peptides tested. The implications of these results on the fusion mechanism of TBEV E protein will be presented.

For all viruses, the first step in replication involves the internalization of a virus particle into a host cell. This process requires that the viral and the host cell membrane fuse, either at the plasma membrane, as is the case for example for HIV-1 (*1*),[1] or after endocytosis (*2*−*5*), as for influenza virus and a number of flaviviruses, such as tick-borne encephalitis virus (TBEV).[2] Viral proteins, known as *fusion proteins*, mediate this fusion event. There are two known classes of fusion proteins, class I and class II, depending on where the sequence responsible for fusion, known as the *fusion peptide*, resides at the N-terminus or aminoproximal end (e.g., influenza, measles, HIV, Ebola (*6*, *7*)) or is an internal segment of the protein, respectively. It is believed that the interaction between the fusion peptide and the lipid membrane is one important event in initiating membrane fusion (*8*). Over the years, a number of class I fusion proteins have been studied extensively, leading to the proposal of a number of fusion mechanisms (*9*−*13*). Of the class II fusion proteins, only a few have been studied to date.

Class II fusion proteins are found in flaviviruses, such as TBEV, yellow fever, West Nile, and dengue virus, and in alphaviruses, such as Semliki Forest and Sindbis viruses. These proteins associate with a second protector protein, the cleavage of which primes the fusion protein to respond to acidic pH. The fusion protein is called E in flaviviruses and E1 in alphaviruses. Structures have been determined for the ectodomains of three class II proteins in their prefusion and postfusion states (*14*−*17*). The structures of the E protein of TBEV and dengue viruses are dimeric in the neutral state and trimeric in the acidic state (*18*−*20*). They have three domains, with folds based largely on β-sheets. Domain II, which contains an elongated, finger-like structure, bears a peptide loop at its tip with a hydrophobic sequence which is highly conserved among all flaviviruses. Experiments on TBEV show that this peptide loop (residues 100−108) is responsible for the attachment of soluble E ectodomains to target membranes and that the hydrophobic residues are essential for fusogenic activity (*21*). Given that residue 101 is a highly conserved Trp, it is possible that residues 100−101 are close to the lipid interface, as shown in studies on other peptides containing Trp (*22*). These and other data, including results from

†The research was supported by the National Sciences Engineering Research Council of Canada.

*To whom correspondence should be addressed. Phone: (604) 822-2537. Fax: (604) 822-2847. E-mail: sstraus@chem.ubc.ca.

[1]There is recent evidence, however, to suggest that HIV-1 also undergoes endocytosis (*75*).

[2]Abbreviations: TBEV, tick-borne encephalitis virus; CD, circular dichroism; FRET, fluorescence resonance energy transfer; HA, hemagglutinin; HIV, human immunodeficiency virus; HBTU, 2-(1*H*-benzotriazol-1-yl)-1,1,3,3-tetramethyluronium hexafluorophosphate; DMF, *N*,*N*-dimethylformamide; DCM, dichloromethane; DIEA, *N*,*N*-diiopropylethylamine; TFA, trifluoroacetic aicd; EDT, ethanedithiol; TES, triethylsilane; Chol, cholesterol; POPC, 1-palmitoyl-2-oleoyl-*sn*-glycero-3-phosphocholine; POPE, 1-palmitoyl-2-oleoyl-*sn*-glycero-3-phosphoethanolamine; NBD-PE, *N*-(7-nitro-2,1,3-benzoxadiazol-4-yl)phosphatidylethanolamine; Rh-PE, *N*-(lissamine Rhodamine B sulfonyl)phosphatidylethanolamine; MALDI, matrix-assisted laser desorption/ionization; RP-HPLC, reserved-phase high-performance liquid chromatography; SUV, small unilamellar vesicles; LUV, large unilamellar vesicles; HEPES, 2-[4-(2-hydroxyethyl)-1-piperazinyl]ethanesulfonic acid.

Published on Web 12/10/2009

studies of alphaviruses (*23*, *24*), which have a very similar peptide loop structure, support the view that the peptide loop of class II fusion proteins has a function analogous to that of the N-terminal fusion peptide in class I fusion proteins: insertion into the host-cell membrane and provision of an attachment point for drawing host membranes together (*6*).

Although the structure of the TBEV E protein yields insight into the mechanism of fusion, there is a lack of direct information on the interaction of the fusion peptide segment with membrane bilayers. To our knowledge, no free synthetic fusion peptide has been used as a model for class II envelope proteins, unlike their class I counterparts, where synthetic fusion peptides have served as useful model fusion systems for structure and activity studies (*8*, *25*−*45*). In the present study, we therefore designed a number of peptides, each encompassing the TBEV fusion peptide sequence, and tested their potential as model fusion systems. Since studies on the E protein showed that the nature of the amino acid at position 107 is important for activity (*21*), we have investigated three peptides consisting of residues 93−113 of the wild-type E protein with Leu at position 107 (WT) and two mutants, namely, L107F and L107T (Figure 1a,c). Data have shown that as the side chain becomes more polar, the fusogenic activity decreases (*21*). In addition, according to the crystal structure of class II fusion protein, the protein adopts a trimeric structure in its fusogenic conformation (Figure 1c) (*17*). We, therefore, synthesized a trimer consisting of three peptides (residues 93−113 of the E protein + K), linked at the C-terminus via the lysine side chain (Figure 1b,c). Finally, since the 93−113 segment is somewhat hydrophobic, we synthesized a version of the peptide with six additional lysine residues attached at the C-terminus (TFPmnK, Figure 1b), in a manner analogous to what was done for the HIV gp41 fusion peptide (*46*). A trimer version of TFPmnK, denoted TFPtrK (Figure 1b), was also made. For all peptides, we investigated secondary structure at neutral (pH 7.5) and acidic (pH 5.5) using circular dichroism (CD). The fusion activities of the peptides were determined by FRET and photon correlation spectroscopy, and their location in the membrane was determined by monitoring tryptophan fluorescence. For the WT, L107F, and L107T, molecular dynamics simulations were also performed to determine how the peptides chains interact in the trimers at the atomic level. Overall, this study will serve to demonstrate whether the fusion peptide of TBEV displays fusogenic activity when investigated on its own and whether the structure correlates to function.

MATERIALS AND METHODS

Materials. Fmoc-protected amino acids, Wang resin, and 2-(1*H*-benzotriazol-1-yl)-1,1,3,3-tetramethyluronium hexafluorophosphate (HBTU) were obtained from Advanced Chemtech (Louisville, KY). *N*,*N*-Dimethylformamide (DMF), dichloromethane (DCM), and acetonitrile were purchased from Fisher (Ottawa, Ontario, Canada). *N*,*N*-Diiopropylethylamine (DIEA), trifluoroacetic aicd (TFA), thioanisole, phenol, ethanedithiol (EDT), triethylsilane (TES), and cholesterol were purchased from Sigma-Aldrich (Oakville, Ontario, Canada). 1-Palmitoyl-2-oleoyl-*sn*-glycero-3-phosphocholine (POPC), 1-palmitoyl-2-oleoyl-*sn*-glycero-3-phosphoethanolamine (POPE), *N*-(7-nitro-2,1,3-benzoxadiazol-4-yl)phosphatidylethanolamine (NBD-PE), and *N*-(lissamine Rhodamine B sulfonyl)phosphatidylethanolamine (Rh-PE) were used as supplied from Avanti Polar Lipids (Alabaster, AL).

a) **WT** K^{93}RDQSDRGWGNHC^{105}G**L**^{107}FGKGSI^{113}

L107F K^{93}RDQSDRGWGNHC^{105}G**F**^{107}FGKGSI^{113}

L107T K^{93}RDQSDRGWGNHC^{105}G**T**^{107}FGKGSI^{113}

b) **TFPmn** K^{93}RDQSDRGWGNHA^{105}GLFGKGSI^{113}

TFPtr K^{93}RDQSDRGWGNHA^{105}GLFGKGSI^{113}KA
K^{93}RDQSDRGWGNHA^{105}GLFGKGSI^{113}K
K^{93}RDQSDRGWGNHA^{105}GLFGKGSI^{113}K

TFPmnK K^{93}RDQSDRGWGNHA^{105}GLFGKGSI^{113}KKKKKK

TFPtrK K^{93}RDQSDRGWGNHA^{105}GLFGKGSI^{113}KKKKKKA
K^{93}RDQSDRGWGNHA^{105}GLFGKGSI^{113}KKKKKK
K^{93}RDQSDRGWGNHA^{105}GLFGKGSI^{113}KKKKKK

c)

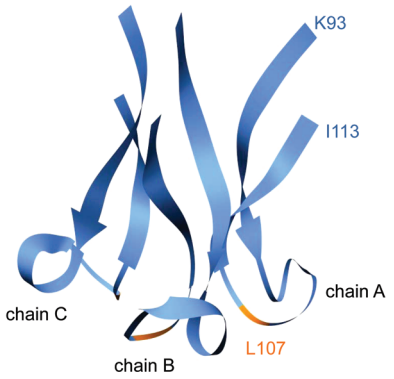

FIGURE 1: Amino acid sequences of the peptides made in this study: (a) monomers consisting of residues 93−113 of the wild-type E protein with Leu at position 107 (WT) and two mutants, namely, L107F and L107T; (b) TFPmn, a monomer consisting of residues 93−113 with a C105A mutation; TFPtr, a trimer consisting of three of these peptides (+K) linked at the C-terminus via the lysine side chain; TFPmnK, a monomer consisting of residues 93−113 with C105A mutation plus six additional lysines at the C-terminus, and, finally, TFPtrK, a trimer consisting of three monomers linked via the side chain of the sixth lysine. (c) Model of the fusion peptide trimer, based on the crystal structure of the full E protein at low pH (1URZ.pdb) (*56*). Residues 93, 113, and 107 are indicated.

Peptide Synthesis. The sequences of the peptides made are given in Figure 1. All of the monomers were synthesized on precoupled Wang resin. To couple the first residue on the Wang resin, Fmoc-protected amino acid (1 mmol) was preactivated for 3 min with 1 mmol of HBTU (0.2 M in DMF) in the presence of 2 mmol of DIEA and coupled overnight to 0.25 mmol of Wang resin. Next, precoupled Wang resin was loaded onto a CS Bio CS136XT peptide synthesizer (Menlo Park, CA) for synthesis by the in situ neutralization Fmoc chemistry. Side-chain protection for the amino acids was as follows: Arg(Pmc), Asn(Trt), Asp(OtBu), Cys(Trt), Gln(Trt), His(Trt), Lys(Boc), Ser(tBu), and Trp(Boc). For double coupling of Lys^{93}, Arg^{94}, and His^{104}, one additional coupling step was performed with only DMF washes in between. After the synthesis was complete, the peptide was deprotected and simultaneously cleaved from the resin using a cleavage mixture composed of 81.5% TFA, 5% thioanisole, 5% phenol, 5% ddH_2O, 2.5% EDT, and 1% TES for 5 h. After evaporation of the TFA under reduced pressure, crude products were precipitated and triturated with chilled diethyl ether, and the peptide products were dissolved in water and then were lyophilized.

The synthesis of trimers began by coupling 0.4 mmol of Fmoc-β-Ala onto 0.1 mmol of Wang resin (*46*). Sequent couplings of

two Fmoc-Lys(Mtt) and one Fmoc-Lys(Boc) formed a lysine trimer backbone. After each addition of Fmoc-Lys(Mtt), the Mtt protection group was removed using a 1:5:94 mixture of TFA:TES:DCM. The 1% TFA deprotection cycle was repeated six times until the TFA solution remained colorless. After the trimer scaffold was completed by the addition of Fmoc-Lys(Boc), the synthesis was then continued on the synthesizer, and the peptide was cleaved from the resin using the same procedure outlined above.

Synthetic peptides were purified by preparative gradient RP-HPLC on a Waters 600 system (Milford, MA), equipped with a Waters 2996 photodiode array detector with 229 nm UV detection using a Phenomenex (Torrance, CA) C4 column (20 μm, 2.1 × 25 cm) at a flow rate of 10 mL/min, with a gradient of 0−50% buffer B (10% ddH_2O, 90% acetonitrile containing 0.1% TFA) in buffer A (90% ddH_2O, 10% acetonitrile containing 0.1% TFA) over 60 min. The purified peptides (>95% purity based on HPLC elution) were lyophilized. The products were characterized by MALDI MS (WT, calculated mass = 2318.5, observed mass = 2318.7; L107F, calculated mass = 2352.5, observed mass = 2352.8; L107T, calculated mass = 2306.0, observed mass = 2306.4; TFPmn, calculated mass = 2286.9, observed mass = 2287.1; TFPtr, calculated mass = 7278.8, observed mass = 7278.7; TFPmnK, calculated mass = 3055.5, observed mass = 3055.6; TFPtrK, calculated mass = 9201.4, observed mass = 9201.8).

Vesicle Preparation. The appropriate lipids were dried using a stream of air to remove most of the chloroform and then vacuum-dried overnight in a 5 mL round-bottom flask. Small unilamellar vesicles (SUVs) were prepared by sonicating the lipids, resuspended in 20 mM phosphate buffer, for 3 h. Large unilamellar vesicles (LUVs), on the other hand, were prepared by resuspending the lipids in 20 mM HEPES buffer. After five freezing and thawing cycles, the lipid suspensions were extruded 10 times through two stacked polycarbonate filters. The LUVs studied by proton correlation spectroscopy were filtered through 0.05 μm pore-size filters, while the samples studied using fluorescence resonance energy transfer (FRET) and tryptophan fluorescence were filtered through 0.1 μm pore-size filters.

CD Spectroscopy. CD spectra were measured using a Jasco J-810 spectropolarimeter (Victoria, British Columbia, Canada). Spectra were recorded from 250 to 195 nm at a sensitivity of 5 mdeg, a resolution of 0.1 nm, a response of 4 s, a bandwidth of 1.0 nm, and a scan speed of 20 nm/min with three accumulations. The peptide concentration in 20 mM phosphate buffer was 50 μM. Phospholipid concentrations of SUVs were 1 mM.

Photon Correlation Spectroscopy. Measurements were carried out on a Beckman Coulter N4plus photon-correlation spectrometer (Mississauga, Ontario, Canada) using a 600 nm laser at 90°. The liposomes (total phospholipids, 26 μM) consisted of POPC, POPE, and cholesterol (molar ratio 1:1:1.5) in a 20 mM HEPES buffer. This high proportion of cholesterol was used in order to compare with data on the E protein (*47*−*49*). The peptides were added into the aqueous liposome solution to give a final concentration of 26 μM for the monomers and 9 μM for the two trimers. Similar results were obtained for peptide-to-lipid ratios of 1:20 and vesicles filtered through 0.1 μm pore-size filters (data not shown). The vesicle sizes were measured after the incubation of the liposome sample at 37 °C for half an hour. The fusion reaction was initiated by the addition of 1 M HCl to yield the appropriate pH.

Fluorescence Resonance Energy Transfer (*FRET*). Measurements were conducted at 37 °C in thermostated cuvettes with constant stirring in a Varian Eclipse fluorescence spectrophotometer (Palo Alto, CA). The assay is based on the dilution of NBD-PE and Rh-PE (*50*). Dilution due to membrane lipid fusion results in a decrease in Rh-PE fluorescence. LUVs containing 1 mol % of each probe were mixed with unlabeled LUVs at a 1:9 ratio with 100 μM total lipid in 2 mL of HEPES buffer at pH 5.0. The Rh-PE emission was monitored at 590 nm, with the excitation wavelength set at 465 nm. The fluorescence scale was calibrated such that the 0% value corresponded to the initial residual fluorescence of the labeled vesicles and the 100% value corresponded to the fluorescence after addition of 20 μL of 10% (v/v) Triton X-100. The monomers and trimers were added to yield a final concentration of 5 or 1.7 μM, respectively.

Tryptophan Fluorescence. In this assay, the peptide−lipid mixtures were incubated at room temperature for 1 h before data acquisition. The final peptide concentrations were 1 or 0.3 μM for the monomers and trimers, respectively, at pH 5.0. Corrected Trp emission spectra were acquired at 37 °C using a Varian Eclipse fluorescence spectrophotometer (Palo Alto, CA). Excitation of the indole ring was set at 280 nm.

Molecular Dynamics Simulations. The GROMOS96 biomolecular simulation package and the 43A1 force field (*51*, *52*) were used. All simulations were performed in explicit SPC water (*53*) under rectangular periodic boundary conditions (box dimensions = 6.60 nm × 6.60 nm × 6.61 nm) in the NPT ensemble (T = 300 K, P = 1 atm) imposed by the Berendsen weak coupling methods (*53*). Covalent bonds were constrained using the SHAKE method (*54*) with a relative geometric tolerance of 10^{-4}. A reaction field long-range correction (*55*) to the truncated Coulomb potential was applied. For the initial coordinates, residues 72−118 from chains A, B, and C (Figure 1c) were taken from the crystal structure of the low pH induced trimer form (1URZ from PDB (*56*)). These residues are located near the tip of domain II and incorporate the fusion peptide (residues 100−113) and 2 disulfides. Initial coordinates for the L107F and L107T mutants were generated by modifying residue 107 into the appropriate residue types using CHIMERA (*57*). This structure was solvated and minimized, after which the system was rendered neutral by the addition of 12 Cl^- ions (number of water molecules = 9012). After a second minimization step, initial atomic velocities were generated from a Maxwell−Boltzmann distribution at 300 K, and the system was equilibrated for 500 ps with positional restraints on all Cα atoms.

A 10 ns simulation was performed starting from this equilibrated system for the WT, L107F, and L107T trimers. Twenty-two residues near the beginning and end of the 72−118 segment (i.e., farthest from the fusion peptide) were position-restrained at the Cα atoms for data collection. This was done to ensure that the trimer does not separate at one end during the course of the simulation.

Two thousand snapshots were used to calculate the total N to N to N distance between the backbone amide atom positions at residue 107. The results were plotted as histograms using gnuplot.

RESULTS

Secondary Structure of the Peptides. Based on the crystal structure of the E protein of TBEV (*14*), the segment consisting of residues 93−113 is expected to consist of 12 residues that adopt β-strand conformation (Figure 1c). Consequently, we fitted the CD curves measured in the 195−250 nm wavelength range (Supporting Information Figures S1 and S2) using the programs

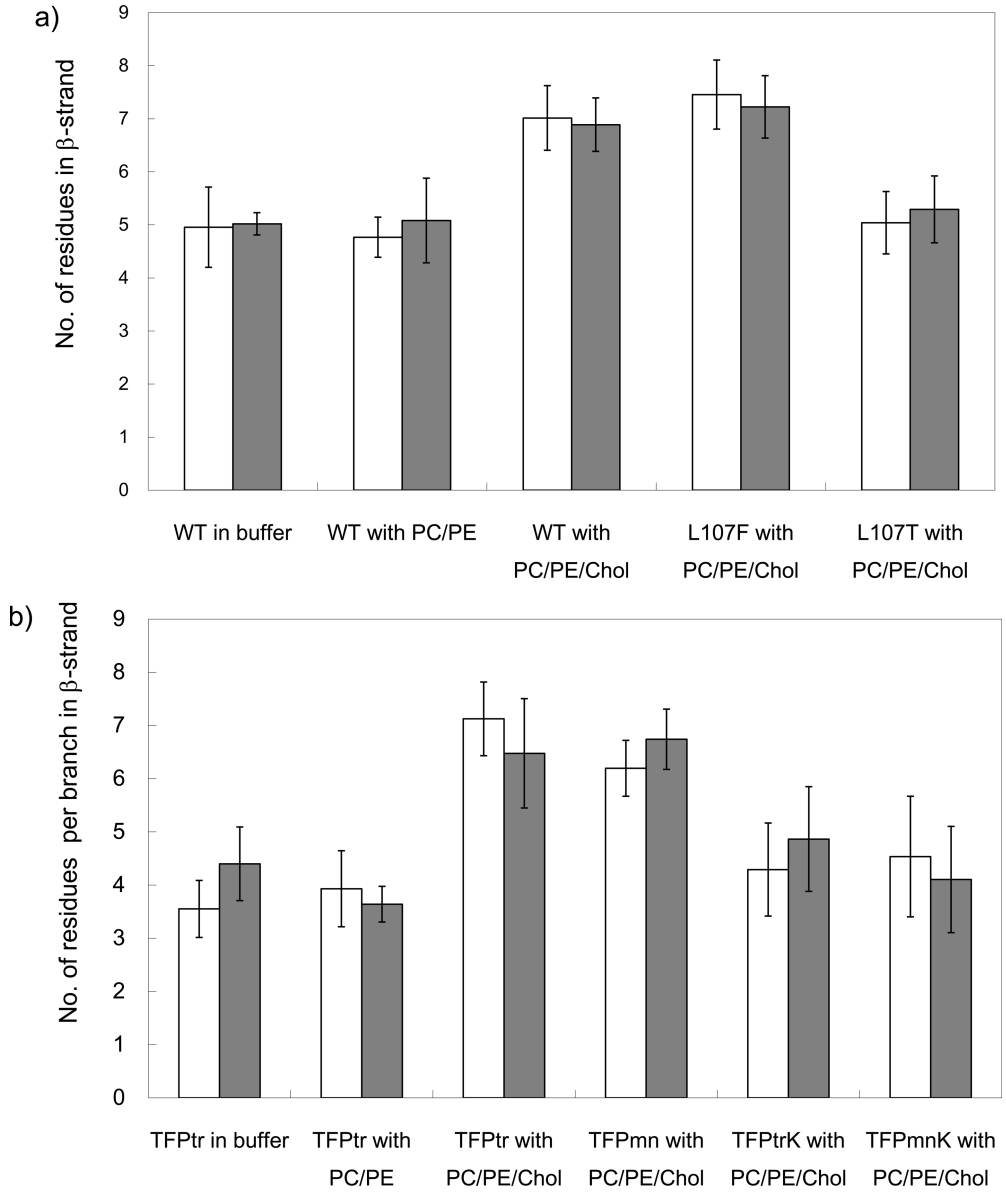

FIGURE 2: Number of residues in the β-strand conformation as obtained from a fit of the CD data (see Supporting Information) of (a) WT, L107F, and L107T and (b) TFPmn, TFPtr, TFPmnK, and TFPtrK. The white bars represent the data obtained at pH 5.0, whereas the gray bars were obtained at pH 7.5. The CD spectra were fitted using the programs CDSSTR (*58*), CONTINLL (*59*), and SELCON3 (*60*), and the number of residues obtained represent an average of the % β-strand content output by these software packages. The error bars represent the standard deviation obtained from the average. The number of residues was obtained by multiplying the percentage by the total number of residues. For the trimers, the results are reported as a number per strand, so that a direct comparison can be made between monomers and trimers.

CDSSTR (*58*), CONTINLL (*59*), and SELCON3 (*60*) and report the number of residues in β-strand conformation for the different peptides under study here in Figure 2. Figure 2a shows that only ca. five residues in the WT peptide adopt β-strand conformation in buffer and in POPC/POPE alone. When cholesterol is added, the peptide adopts slightly more β-strand structure. This is consistent with findings reported for the HIV fusion peptide that cholesterol promotes β-strand structure (*45*). The fusion peptide of HIV adopts an uninterrupted β-strand conformation in the presence of cholesterol (*45*) and a helical structure in its absence (*30*). Interestingly, there is no significant increase in secondary structure as a function of pH. This is in sharp contrast to the fusion peptide of hemagglutinin, which shows a pH-dependent conformational change (*61*). A comparison of WT with L107F and L107T illustrates that WT and L107F adopt similar degrees of secondary structure, whereas L107T is less structured. Figure 2b shows the results for the TFPmn, TFPtr, TFPmnK, and TFPtrK. Here again, cholesterol helps to promote the β-strand conformation, as seen by the increase in the number of residues in this conformation for TFPtr. The mutation from Cys to Ala at position 105 has no effect on the secondary structure as the data for WT (Figure 2a) and TFPmn (Figure 2b) are similar. Finally, the presence of the six Lys tag at the C-terminus appears to perturb the secondary structure, as seen in Figure 2b.

Fusion Activity of the Peptides. Two different methods were used to determine the fusogenic activity of the peptides under study. In photon correlation spectroscopy (Figure 3), the sizes of vesicles consisting of POPC/POPE/cholesterol (1:1:1.5 molar ratio) were measured as a function of pH. Because fusion induced by the peptides causes vesicle aggregation, the increase in the mean diameter of LUVs when peptide is added indicates fusion. As a control, the size of POPC/POPE/cholesterol vesicles alone was measured, as a function of pH. It was found that the

size remains constant (data not shown). Next, the vesicles were incubated with the peptides for half an hour, and the aggregation was then measured as a function of pH. Figure 3a compares the results obtained for WT, L107F, and L107T. At pH 5.5, which is the optimum fusion pH for the TBEV E protein (*62*), the diameter of the POPC/POPE/cholesterol vesicles was found to increase by a factor of 1.7, 1.6, and 1.2 in the presence of WT, L10F, and L107T. These results indicated that replacement of the Leu107 residue with the hydrophilic amino acid Thr strongly impaired fusogenic activity, whereas the Phe mutant still retained a significant degree of fusogenic activity, consistent with the data obtained for reconstituted viral particles containing E protein with the same mutations (*62*). Interestingly, in the peptides studied here, the fusogenic activity continued to increase as the pH was lowered, suggesting that the pH optimum is shifted to more acidic pH values. In Figure 3b, the mean diameters measured for vesicles incubated with TFPtr (black solid line), TFPmn (black dashed line), TFPtrK (gray solid line), and TFPmnK (gray dashed line) are shown as a function of pH. It was found that the mean diameter of the POPC/POPE/cholesterol vesicles increase by a factor of 1.7, 2.2, 1.4, and 1.3 for TFPmn, TFPtr, TFPmnK, and TFPtrK in going from pH 7.0 to pH 5.0. The data also show that the fusion activities of WT and C105A are similar, indicating that the mutation did not have significant impact on fusogenicity. A comparison of TFPmn with TFPtr shows that the trimer is more active over the entire pH range, suggesting that trimer formation is important for activity. Note that since the trimers have three times as many strands per molecule as their monomers, the concentrations of trimers used were one-third of those of monomers. Finally, the peptides containing six Lys, TFPmnK and TFPtrK, are both very active, even at neutral pH. The increased net charge of these peptides, as compared to those that only contain one Lys residue at the C-terminus, may promote vesicle content mixing and content leakage (*63*, *64*).

Fusion activity was also monitored by using FRET (Figure 4). In this assay, the final extent of lipid mixing was used as a general measure of peptide fusogenicity. In Figure 4a, the results shown for WT (black solid line), L107F (black dotted line), and L107T (gray solid line) follow the same trends as obtained from the photon correlation spectroscopy, described above. These data also agree with findings reported for reconstituted viral particles which contain the whole E protein with either a Leu, Phe, or Thr at position 107 (*62*). Likewise, the data in Figure 4b for TFPtr (black solid line), TFPmn (black dotted line), TFPtrK (gray solid line), and TFPmnK (gray dotted line) support the findings from the photon correlation spectroscopy. Here again, the trimers are more active than the monomers, and the peptides containing six Lys residues at the C-terminus are more active, even prior to acidification of the sample. For the latter four peptides, the extent of fusion was fitted using the equation (*41*):

$$M(t) = M_0 + M_1(1 - e^{-k_1 t}) + M_2(1 - e^{-k_2 t})$$

where M_0 represents the extent of fusion prior to adding acid, and the induced fusion increase after acidification is modeled as the sum of a fast buildup with overall induced fusion M_1 and rate constant k_1 and a slow buildup with overall induced fusion M_2 and rate constant k_2. The resulting parameters are listed in Table S1 in the Supporting Information. For TFPtr and TFPmn, M_0 was around zero, whereas for the six Lys-containing constructs, it was large, indicating that fusion occurs already at neutral pH for TFPmnK and TFPtrK. A comparison of k_1 for TFPtr and

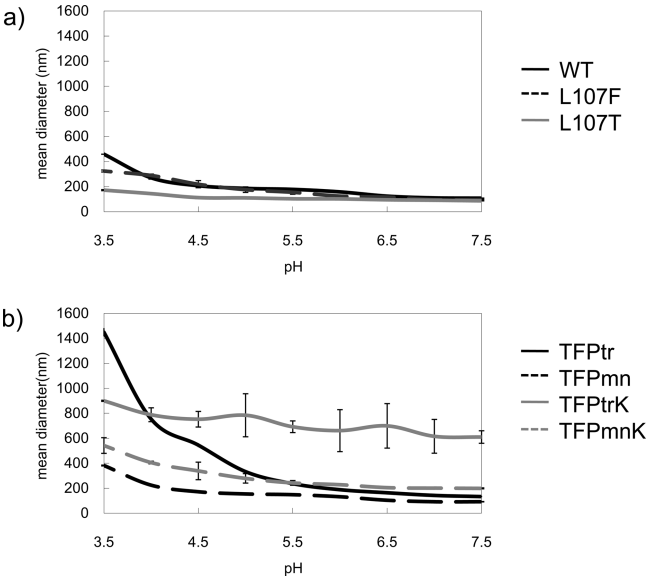

FIGURE 3: Mean diameter of lipid vesicles composed of POPC/POPE/cholesterol (molar ratio 1:1:1.5) as function of pH from photon correlation spectroscopy. In (a), the vesicles were incubated with WT (black solid line), L107F (black dashed line), and L107T (gray solid line) for 30 min prior to the measurements. In (b), the vesicles were incubated with TFPtr (black solid line), TFPmn (black dashed line), TFPtrK (gray solid line), and TFPmnK (gray dashed line). The *y*-axes in (a) and (b) are plotted on the same scale for comparison. The errors bars indicate the standard deviation obtained from three repeat measurements.

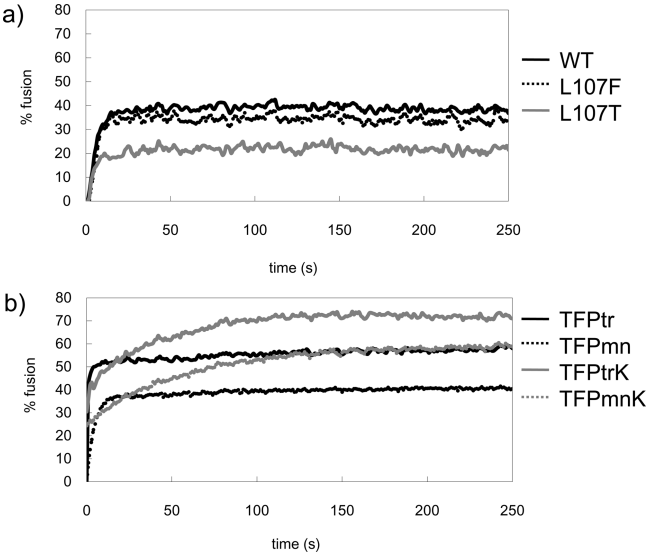

FIGURE 4: Percent fusion measured as a function of time using FRET for (a) WT (black solid line), L107F (black dotted line), and L107T (gray solid line) and (b) TFPtr (black solid line), TFPmn (black dotted line), TFPtrK (gray solid line), and TFPmnK (gray dotted line). Time zero represents the time at which the samples were acidified (pH 5.0).

TFPmn shows that the rate constant is 9 times larger for the trimer (1.63 versus 0.19 s^{-1}). This is in contrast to studies on the fusion peptide from HIV which showed that the peptide trimer induces fusion at a rate which is up to 40 times larger than the corresponding rate for the HIV fusion peptide monomer (*41*). Nevertheless, the data show that the trimer of TBEV is more fusogenic than the monomer, and the fast rate determined for TBEV, as compared to that obtained for the HIV fusion peptide

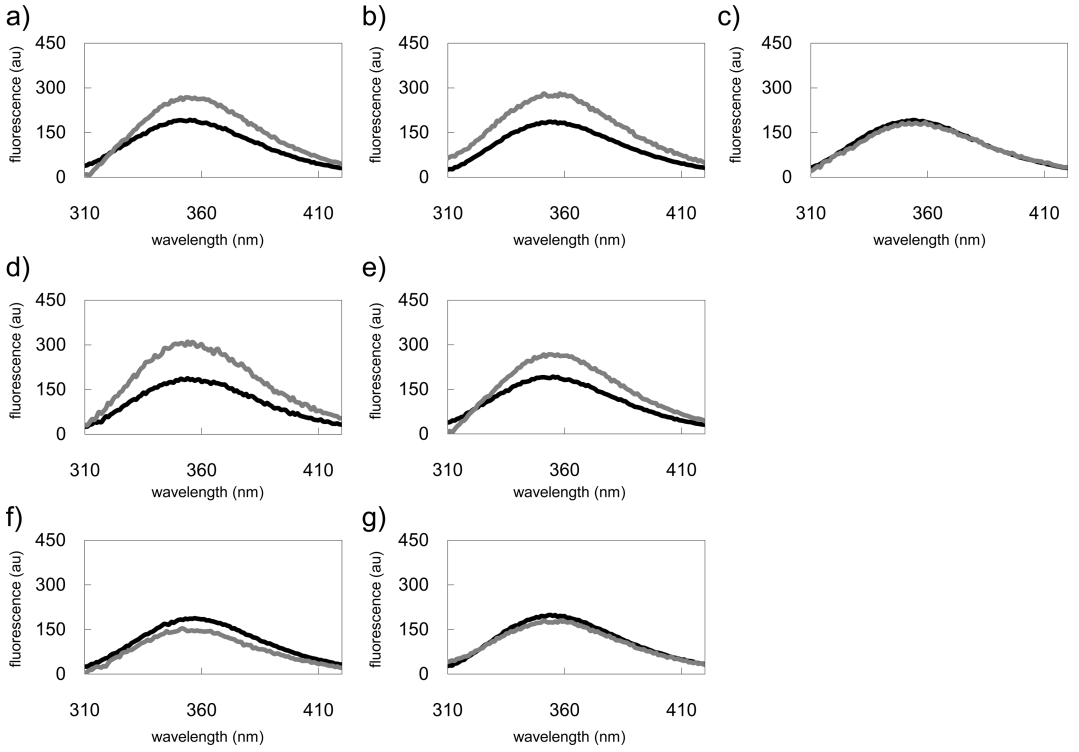

FIGURE 5: Fluorescence emission spectra of the Trp101 residue in (a) WT, (b) L107F, (c) L107T, (d) TFPtr, (e) TFPmn, (f) TFPmnK, and (g) TFPtrK in 20 mM HEPES buffer at pH 5.5 (black solid line) and incubated with POPC/POPE/cholesterol LUVs with peptide-to-lipid ratios of 1:100 for the monomers and 1:300 for the trimers (gray solid line). The wavelengths of maximum emission are (a) WT at pH 5.5 in buffer λ_{max} = 357 nm and in lipid λ_{max} = 356 nm, (b) L107F at pH 5.5 in buffer λ_{max} = 356 nm and in lipid λ_{max} = 354 nm, (c) L107T at pH 5.5 in buffer λ_{max} = 355 nm and in lipid λ_{max} = 355 nm, (d) TFPtr at pH 5.5 in buffer λ_{max} = 357 nm and in lipid λ_{max} = 354 nm, (e) TFPmn at pH 5.5 in buffer λ_{max} = 356 nm and in lipid λ_{max} = 356 nm, (f) TFPmnK at pH 5.5 in buffer λ_{max} = 358 nm and in lipid λ_{max} = 358 nm, and (g) TFPtrK at pH 5.5 in buffer λ_{max} = 357 nm and in lipid λ_{max} = 357 nm.

trimer (0.43 s^{-1}) (*41*), is consistent with data for E proteins (*33*, *62*). Interestingly, the parameters for TFPmnK and TFPtrK show that the slow buildup with overall induced fusion M_2 and rate constant k_2 dominates.

Peptide Penetration. The fluorescence of the Trp101 residue in the various fusion peptides studied here was used to gain some insight into whether these peptides penetrate the membrane bilayer. In Figure 5 the emission spectra of the peptides in buffer and in the presence of lipid LUVs are compared. The WT peptide inserts into the POPC/POPE/cholesterol membranes at pH 5.5 (Figure 5a) and less so at pH 7.5 (Supporting Information Figure S3). In the absence of cholesterol, there is no insertion of the Trp into the membrane bilayer, suggesting that cholesterol is essential for peptide−lipid interactions. A comparison of WT with L107F (Figure 5b) and L107T (Figure 5c) clearly indicates that WT and L107F can interact with the membrane, whereas the presence of the polar residue Thr in the L107T mutant hinders any interactions. Panels d and e of Figure 5 indicate that the TFPtr and TFPmn both interact with the POPC/POPE/cholesterol membranes in a manner similar to the WT. The addition of six Lys at the C-terminus, however, perturbs the peptide−lipid interaction. The increased solubility afforded by the addition of six Lys residues may cause TFPmnK and TFPtrK to preferentially partition into the solvent.

MD Simulations of the WT, L107F, and L107T Trimers. The molecular dynamics simulations were performed on the WT, L107F, and L107T trimers to gain insight into how the mutation affects trimer stability. The simulations were performed by position restraining residues far from the fusion peptide segment, to ensure that the trimer would not fall apart completely. The fusion peptide segment, however, was not restrained. As the data in Figure 6 show, both the WT and L107F maintain a similar backbone N to N to N distance at position 107. The (N at 107)$_{chain1}$ + (N at 107)$_{chain2}$ + (N at 107)$_{chain3}$ distance for L107T, on the other hand, increased during the course of the simulation, indicating that the chains were being pushed apart by the presence of a polar residue. A simulation of L107D, which has been shown to have no fusion activity whatsoever (*62*), showed similar trends, with even larger chain−chain distances being sampled during the simulation (data not shown).

DISCUSSION

In order to understand how fusion proteins mediate fusion between the viral and host cell membranes, the fusion protein, or the short segment known as the *fusion peptide*, can be studied. The first advantage of using the fusion peptide alone is that it is active, so the synthetic peptide made can be tested for biological relevance. The second advantage of using a peptide over the much larger fusion protein is that the peptide can be investigated in model membranes (e.g., POPC/POPE/cholesterol) directly. This provides unique mechanistic insight into how the fusion peptide inserts into membranes. Used in combination with data on the fusion protein structure, for instance, a full mechanism of membrane fusion can be elucidated. This approach has been used successfully over the years to study the class I fusion proteins from HIV and influenza (*9*−*13*). To our knowledge, an analogous approach for class II fusion proteins has not been used, although there are a number of structural studies that have been conducted on the dengue virus envelope protein and the TBEV E protein (*14*, *49*, *65*).

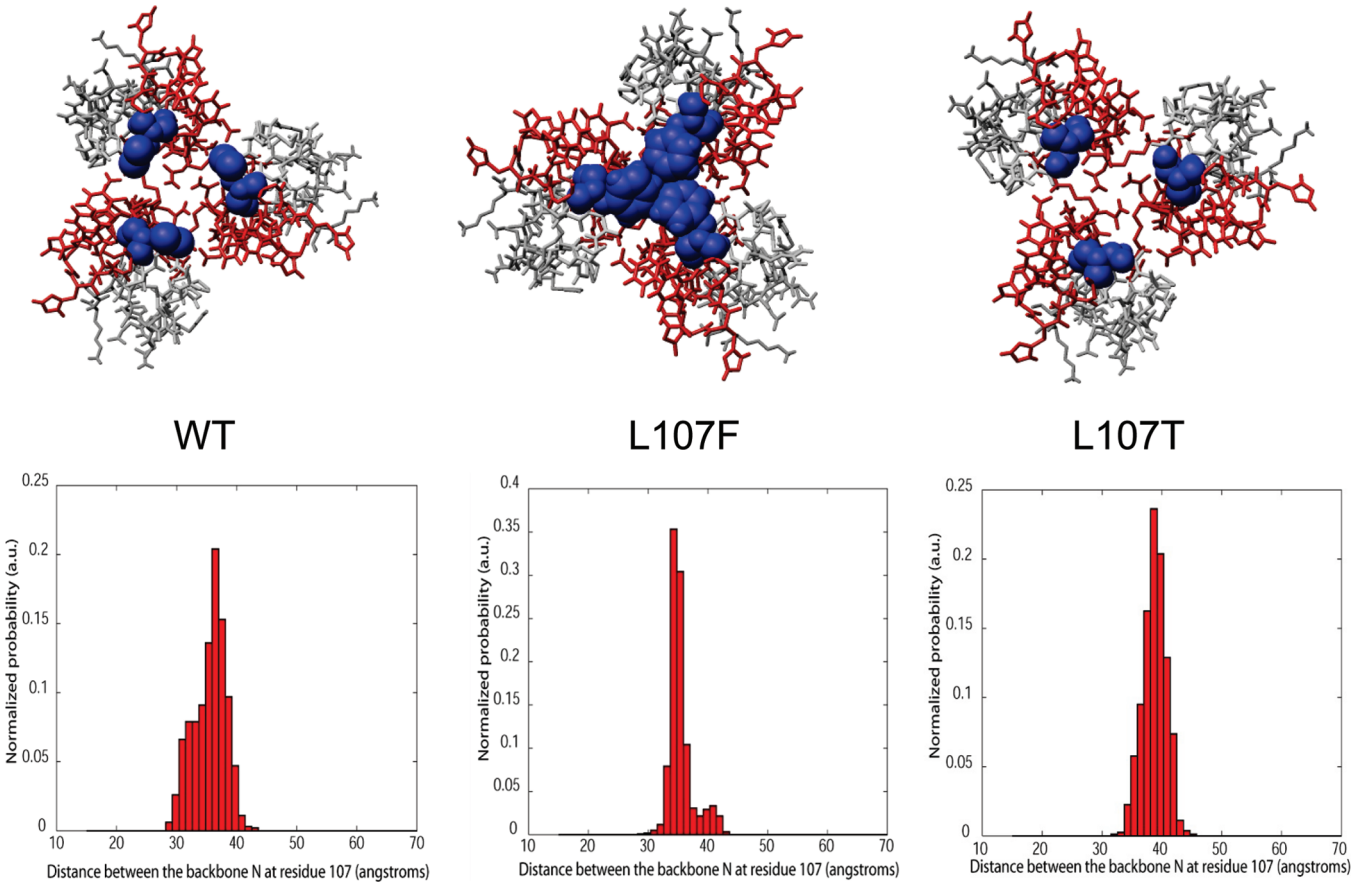

FIGURE 6: Starting structures for the WT, L107F, and L107T fusion peptides for the MD simulations, with identical backbone N to N to N distance (i.e., constant $(N \text{ at } 107)_{chain1} + (N \text{ at } 107)_{chain2} + (N \text{ at } 107)_{chain3}$). The red segment represents residues 93−113. Residue 107 is shown in blue/CPK. The panels below represent the distance measured between the amide N for residue 107 during the course of the 10 ns MD simulations in explicit water.

In this paper, we have therefore investigated a number of synthetic fusion peptide constructs derived from the TBEV E protein to determine, on one hand, whether such peptides can be active on their own and, on the other, to try to understand which parameters (e.g., sequence, structure, trimer formation, or peptide−lipid interactions) are important for fusion. We have therefore made the following constructs to better understand the mechanism of fusion induced by the flavivirus E protein (*14*, *49*, *65*): (1) monomers consisting of residues 93−113 of the wild-type TBEV E protein with Leu at position 107 (WT) and two mutants, namely, L107F and L107T; (2) TFPmn, a monomer consisting of residues 93−113 of the E protein with a C105A mutation; (3) TFPtr, a trimer consisting of three monomers described in (2), linked at the C-terminus via one Lys; (4) TFPmnK, a monomer consisting of residues 93−113 of the E protein plus six additional Lys at the C-terminus; and (5) TFPtrK, a trimer consisting of three monomers described in (3), linked via the side chain of the sixth lysine.

Structure and Activity of WT and TFPmn. As the data show, the WT peptide can induce fusion of POPC/POPE/cholesterol vesicles at acidic pH despite possessing less secondary structure than the corresponding segment in the E protein. Given that the E protein is stabilized by a number of disulfide bonds (Cys91−Cys116, Cys74−Cys105), the loss of some secondary structure is not surprising. Data on a peptide consisting of residues G89−A119 with a mutation at C105 and possessing the disulfide at C91−C119 does indeed contain a higher proportion of β-strand structure (45%) than the WT (33%) (data not shown). Interestingly though, this longer peptide displays the same extent of fusion (40%) as the WT and penetrates membranes to the same extent. Since the fusion peptide itself is in the loop segment at residues 100−108, these results suggest that, although the disulfides serve to stabilize the structure away from the fusion peptide segment, this has no effect on the loop itself, which is most likely the part that interacts directly with the lipids and is responsible for fusion. When compared to data obtained on pyrene-labeled TBEV virus (*62*), the WT peptide is less effective at promoting fusion and does so at a slower rate. This suggests that trimerization of the fusion peptide segment (see below) or interactions between the fusion peptide and other parts of the E protein may be critical for optimal fusion activity. The data also show the importance of cholesterol for activity. In the absence of cholesterol, the peptide does not insert into membranes effectively. Indeed, the extent of fusion and of insertion increases gradually with an increased proportion of cholesterol (data not shown). This suggests that cholesterol may play a role by modulating the properties of the membrane (e.g., by increasing the lateral packing density and the conformational order of the lipid chains (*66*−*71*)) or by a direct interaction between the peptide and cholesterol (*18*). Finally, the data on the C105A mutant show that a mutation at this position has only minor effects on structure and activity.

Comparison between WT and L107F/*L107T*. As the data show, mutation at the highly conserved residue 107 has an effect on secondary structure and activity. The L107F mutation, which can occur in some flaviviruses (e.g., dengue 2 virus E

protein (*58*)), does not have a dramatic impact on structure, trimer stability, and therefore activity. The L107T mutation, on the other hand, results in a fusion peptide with less β-strand structure and a trimer where the fusion peptide loop is pushed further apart. This increased distance between the loops in the trimer is even more dramatic for the L107D mutant. This suggests that there is an optimal arrangement of the trimer which maximizes peptide−lipid interactions. The lack of interaction between the L107T mutant and the POPC/POPE/cholesterol vesicles at a peptide-to-lipid ratio of 1:100 supports this. The residual fusion activity observed for L107T at P/L ratios of 1:20, however, suggests that the fluorescence may be concentration dependent (as observed in Supporting Information Figure S3 for TFPtr).

Comparison between TFPmn and TFPtr. Forming an artificial trimer, held together at what would effectively be residue 114, does not have an effect on secondary structure but has a significant effect on fusion activity. The extent of fusion between TFPmn and TFPtr increases from 35% to 60%, and the rate for the fast fusion component (k) increases by a factor of 9. This suggests that having three fusion peptide loops in close proximity in TFPtr is advantageous for fusion. Presumably in TFPmn, trimer formation is required for fusion, but this process is limited by the rate of diffusion of the monomer in the lipids.

Effect of Adding More Lysines at the C-Terminus. For the hydrophobic hemagglutinin fusion peptide from influenza virus, a number of studies were conducted using a host−guest peptide system, consisting of the fusion peptide sequence and a polar carrier peptide via a flexible linker linked at the C-terminus of FP segment. The polar carrier typically contained a number of lysine residues to improve the solubility of the hemagglutinin fusion peptide (*72*, *73*). Although the TBEV fusion peptide is not as hydrophobic as its hemagglutinin counterpart (GRAVY (*74*) = −1.186 for WT; GRAVY (*74*) = 0.555 for hemagglutinin fusion peptide), we have investigated the effect of making the peptide more soluble on secondary structure and activity. As the data show, adding the six Lys tag at the C-terminus reduces the amount of β-strand conformation and the ability of the peptides to insert into membranes, yet surprisingly the fusion activity of these peptides is the largest of all of those studied here. Activity is even detected at neutral pH. The fact that POPC/POPE/cholesterol vesicles fuse in the presence of TFPmnK and TFPtrK most likely has nothing to do with the fusion peptide segment itself, but rather with the high cationic charge of these two constructs in particular. Indeed, a number of studies have shown that adding large amounts of cholesterol to vesicles containing choline and amino phospholipids affects the initial rates of vesicle content mixing and content leakage in the presence of divalent cations (*63*, *64*).

Effect of pH. For all of the peptides studied here, pH has little effect on the secondary structure as determined by CD. The pH does, however, play a role in the ability of the peptides to insert into lipid membranes, as seen for WT and TFPtr (Supporting Information). Given that the sequence has a His at position 104 and that the pK_a of the His side chain is typically 6.0−6.1, at acidic pH the histidine side chain will be protonated and will most likely prefer to stay nearer to the surface of the lipid bilayer. The small differences observed in the fluorescence at pH 5.5 and 7.5 indicate that the protonation state of His104 does not outright inhibit the peptide's ability to bind to the membrane. Further more detailed studies which pinpoint the exact location of the fusion peptide loop in lipid membranes (e.g., using spin labels) would be needed to quantify the importance of this and other residues in the fusion peptide−lipid interaction.

In summary, we have designed a number of peptides containing the TBEV fusion peptide sequence. Overall, the data show that these peptides can be used as model systems to shed light into the mechanism of fusion for class II fusion proteins. The results demonstrate that trimer formation is essential for activity and are complementary to studies on the E protein from TBEV (*14*, *18*, *21*, *48*, *49*, *62*).

ACKNOWLEDGMENT

We would like to thank a number of people for access to instrumentation used in this study: Melissa Elliott for the fluorescence spectrophotometer and extruder, Fred Rosell for the Jasco J-810 CD spectropolarimeter, and Johan Janzen for the Beckman Coulter N4plus photon-correlation spectrometer. The last two instruments are part of the Laboratory for Molecular Biophysics at the University of British Columbia, a project funded by the Canada Foundation for Innovation.

SUPPORTING INFORMATION AVAILABLE

CD spectra and fluorescence emission spectra of the peptides studied here, as well as the parameters derived from fitting the FRET data. This material is available free of charge via the Internet at http://pubs.acs.org.

REFERENCES

1. Turner, B. G., and Summers, M. F. (1999) Structural biology of HIV. *J. Mol. Biol. 285*, 1–32.
2. Hernandez, L. D., Hoffman, L. R., Wolfsberg, T. G., and White, J. M. (1996) Virus-cell and cell-cell fusion. *Annu. Rev. Cell Dev. Biol. 12*, 627–661.
3. Blumenthal, R., and Dimitrov, D. S. (1997) in Handbook of Physiology, Section 14: Cell Physiology (Hoffman, J. F., and Jamieson, J. C., Eds.) pp 563−603, Oxford, New York.
4. Dimitrov, D. S. (2000) Cell biology of virus entry. *Cell 101*, 697–702.
5. Eckert, D. M., and Kim, P. S. (2001) Mechanisms of viral membrane fusion and its inhibition. *Annu. Rev. Biochem. 70*, 777–810.
6. Skehel, J. J., and Wiley, D. C. (2000) Receptor binding and membrane fusion in virus entry: the influenza hemagglutinin. *Annu. Rev. Biochem. 69*, 531–569.
7. Wilson, I. A., Skehel, J. J., and Wiley, D. C. (1981) Structure of the haemagglutinin membrane glycoprotein of influenza virus at 3 Å resolution. *Nature 289*, 366–373.
8. Durell, S. R., Martin, I., Ruysschaert, J. M., Shai, Y., and Blumenthal, R. (1997) What studies of fusion peptides tell us about viral envelope glycoprotein-mediated membrane fusion (review). *Mol. Membr. Biol. 14*, 97–112.
9. Baker, K. A., Dutch, R. E., Lamb, R. A., and Jardetzky, T. S. (1999) Structural basis for paramyxovirus-mediated membrane fusion. *Mol. Cell 3*, 309–319.
10. Melikyan, G. B., Markosyan, R. M., Hemmati, H., Delmedico, M. K., Lambert, D. M., and Cohen, F. S. (2000) Evidence that the transition of HIV-1 gp41 into a six-helix bundle, not the bundle configuration, induces membrane fusion. *J. Cell Biol. 151*, 413–423.
11. Russell, C. J., Jardetzky, T. S., and Lamb, R. A. (2001) Membrane fusion machines of paramyxoviruses: capture of intermediates of fusion. *EMBO J. 20*, 4024–4034.
12. Bullough, P. A., Hughson, F. M., Skehel, J. J., and Wiley, D. C. (1994) Structure of influenza haemagglutinin at the pH of membrane fusion. *Nature 371*, 37–43.
13. Chen, J., Skehel, J. J., and Wiley, D. C. (1999) N- and C-terminal residues combine in the fusion-pH influenza hemagglutinin HA(2) subunit to form an N cap that terminates the triple-stranded coiled coil. *Proc. Natl. Acad. Sci. U.S.A. 96*, 8967–8972.
14. Rey, F. A., Heinz, F. X., Mandl, C., Kunz, C., and Harrison, S. C. (1995) The envelope glycoprotein from tick-borne encephalitis virus at 2 Å resolution. *Nature 375*, 291–298.
15. Lescar, J., Roussel, A., Wien, M. W., Navaza, J., Fuller, S. D., Wengler, G., and Rey, F. A. (2001) The fusion glycoprotein shell of

Semliki Forest virus: an icosahedral assembly primed for fusogenic activation at endosomal pH. *Cell 105*, 137–148.
16. Modis, Y., Ogata, S., Clements, D., and Harrison, S. D. (2003) A ligand-binding pocket in the dengue virus envelope glycoprotein. *Proc. Natl. Acad. Sci. U.S.A. 100*, 6986–6991.
17. Modis, Y., Ogata, S., Clements, D., and Harrison, S. C. (2004) Structure of the dengue virus envelope protein after membrane fusion. *Nature 427*, 313–319.
18. Allison, S. L., Schalich, J., Stiasny, K., Mandl, C. W., Kunz, C., and Heinz, F. X. (1995) Oligomeric rearrangement of tick-borne encephalitis virus envelope proteins induced by an acidic pH. *J. Virol. 69*, 695–700.
19. Ferlenghi, I., Clarke, M., Rutten, T., Allison, S. L., Schalich, J., Heinz, F. X., Harrison, S. C., Rey, F. A., and Fuller, S. D. (2001) Molecular organization of a recombinant subviral particle from tick-borne encephalitis virus. *Mol. Cell 7*, 593–602.
20. Kuhn, R. J., Zhang, W., Rossmann, M. G., Pletnev, S. V., Corver, J., Lenches, E., Jones, S. T., Mukhopadhyay, S., Chipman, P. R., Strauss, E. G., Baker, T. S., and Strauss, J. H. (2002) Structure of dengue virus: implications for flavivirus organization, maturation, and fusion. *Cell 108*, 717–725.
21. Allison, S. L., Schalich, J., Stiasny, K., Mandl, C. W., and Heinz, F. X. (2001) Mutational evidence for an internal fusion peptide in flavivirus envelope protein E. *J. Virol. 75*, 4268–4275.
22. Raghuraman, H., and Chattopadhyay, A. (2004) Interaction of melittin with membrane cholesterol: a fluorescence approach. *Biophys. J. 87*, 2419–2432.
23. Levy-Mintz, P., and Kielian, M. (1991) Mutagenesis of the putative fusion domain of the Semliki Forest virus spike protein. *J. Virol. 65*, 4292–4300.
24. Ahn, A., Gibbons, D. L., and Kielian, M. (2002) The fusion peptide of Semliki Forest virus associates with sterol-rich membrane domains. *J. Virol. 76*, 3267–3275.
25. Freed, E. O., Myers, D. J., and Risser, R. (1990) Characterization of the fusion domain of the human immunodeficiency virus type 1 envelope glycoprotein gp41. *Proc. Natl. Acad. Sci. U.S.A. 87*, 4650–4654.
26. Freed, E. O., Delwart, E. L., Buchschacher, G. L., Jr., and Panganiban, A. T. (1992) A mutation in the human immunodeficiency virus type 1 transmembrane glycoprotein gp41 dominantly interferes with fusion and infectivity. *Proc. Natl. Acad. Sci. U.S.A. 89*, 70–74.
27. Schaal, H., Klein, M., Gehrmann, P., Adams, O., and Scheid, A. (1995) Requirement of N-terminal amino acid residues of gp41 for human immunodeficiency virus type 1-mediated cell fusion. *J. Virol. 69*, 3308–3314.
28. Delahunty, M. D., Rhee, I., Freed, E. O., and Bonifacino, J. S. (1996) Mutational analysis of the fusion peptide of the human immunodeficiency virus type 1: identification of critical glycine residues. *Virology 218*, 94–102.
29. Pecheur, E., Sainte-Marie, J., Bienvenue, A., and Hoekstra, D. (1999) Peptides and membrane fusion: towards an understanding of the molecular mechanism of protein-induced fusion. *J. Membr. Biol. 167*, 1–17.
30. Rafalski, M., Lear, J. D., and DeGrado, W. F. (1990) Phospholipid interactions of synthetic peptides representing the N-terminus of HIV gp41. *Biochemistry 29*, 7917–7922.
31. Slepushkin, V. A., Melikyan, G. B., Sidorova, M. S., Chumakov, V. M., Andreev, S. M., Manulyan, R. A., and Karamov, E. V. (1990) Interaction of human immunodeficiency virus (HIV-1) fusion peptides with artificial lipid membranes. *Biochem. Biophys. Res. Commun. 172*, 952–957.
32. Martin, I., Defrise-Quertain, F., Decroly, E., Vandenbranden, M., Brasseur, R., and Ruysschaert, J. M. (1993) Orientation and structure of the NH_2-terminal HIV-1 gp41 peptide in fused and aggregated liposomes. *Biochim. Biophys. Acta 1145*, 124–133.
33. Nieva, J. L., Nir, S., Muga, A., Goni, F. M., and Wilschut, J. (1994) Interaction of the HIV-1 fusion peptide with phospholipid vesicles: different structural requirements for fusion and leakage. *Biochemistry 33*, 3201–3209.
34. Mobley, P. W., Lee, H. F., Curtain, C. C., Kirkpatrick, A., Waring, A. J., and Gordon, L. M. (1995) The amino-terminal peptide of HIV-1 glycoprotein 41 fuses human erythrocytes. *Biochim. Biophys. Acta 1271*, 304–314.
35. Martin, I., Schaal, H., Scheid, A., and Ruysschaert, J. M. (1996) Lipid membrane fusion induced by the human immunodeficiency virus type 1 gp41 N-terminal extremity is determined by its orientation in the lipid bilayer. *J. Virol. 70*, 298–304.
36. Kliger, Y., Aharoni, A., Rapaport, D., Jones, P., Blumenthal, R., and Shai, Y. (1997) Fusion peptides derived from the HIV type 1 glycoprotein 41 associate within phospholipid membranes and inhibit cell-cell fusion. Structure-function study. *J. Biol. Chem. 272*, 13496–13505.
37. Pereira, F. B., Goni, F. M., Muga, A., and Nieva, J. L. (1997) Permeabilization and fusion of uncharged lipid vesicles induced by the HIV-1 fusion peptide adopting an extended conformation: dose and sequence effects. *Biophys. J. 73*, 1977–1986.
38. Nieva, J. L., Nir, S., and Wilschut, J. (1998) Destabilization and fusion of zwitterionic large unilamellar lipid vesicles induced by a beta-type structure of the HIV-1 fusion peptide. *J. Liposome Res. 8*, 165–182.
39. Pritsker, M., Rucker, J., Hoffman, T. L., Doms, R. W., and Shai, Y. (1999) Effect of nonpolar substitutions of the conserved Phe11 in the fusion peptide of HIV-1 gp41 on its function, structure, and organization in membranes. *Biochemistry 38*, 11359–11371.
40. Agirre, A., Flach, C., Goñi, F. M., Mendelsohn, R., Valpuesta, J. M., Wu, F., and Nieva, J. L. (2000) Interactions of the HIV-1 fusion peptide with large unilamellar vesicles and monolayers. A cryo-TEM and spectroscopic study. *Biochim. Biophys. Acta 1467*, 153–164.
41. Yang, R., Yang, J., and Weliky, D. P. (2003) Synthesis, enhanced fusogenicity, and solid state NMR measurements of cross-linked HIV-1 fusion peptides. *Biochemistry 42*, 3537–3535.
42. Bodner, M. L., Gabrys, C. M., Parkanzky, P. D., Yang, J., Duskin, C. A., and Weliky, D. P. (2004) Temperature dependence and resonance assignment of ^{13}C NMR spectra of selectively and uniformly labeled fusion peptides associated with membranes. *Magn. Reson. Chem. 24*, 187–194.
43. Wasniewski, C. M., Parkanzky, P. D., Bodner, M. L., and Weliky, D. P. (2004) Solid-state nuclear magnetic resonance studies of HIV and influenza fusion peptide orientations in membrane bilayers using stacked glass plate samples. *Chem. Phys. Lipids 132*, 89–100.
44. Zheng, Z., Yang, R., Bodner, M. L., and Weliky, D. P. (2006) Conformational flexibility and strand arrangements of the membrane-associated HIV fusion peptide trimer probed by solid-state NMR spectroscopy. *Biochemistry 45*, 12960–12975.
45. Qiang, W., Yang, J., and Weliky, D. P. (2007) Solid-state nuclear magnetic resonance measurements of HIV fusion peptide to lipid distances reveal the intimate contact of beta strand peptide with membranes and the proximity of the Ala-14-Gly-16 region with lipid headgroups. *Biochemistry 46*, 4997–5008.
46. Yang, R., Prorok, M., Castellino, F. J., and Weliky, D. P. (2004) A trimeric HIV-1 fusion peptide construct which does not self-associate in aqueous solution and which has 15-fold higher membrane fusion rate. *J. Am. Chem. Soc. 126*, 14722–14723.
47. Stiasny, K., Allison, S. L., Marchler-Bauer, A., Kunz, C., and Heinz, F. X. (1996) Structural requirements for low-pH-induced rearrangements in the envelope glycoprotein of tick-borne encephalitis virus. *J. Virol. 70*, 8142–8147.
48. Stiasny, K., Koessl, C., and Heinz, F. X. (2003) Involvement of lipids in different steps of the flavivirus fusion mechanism. *J. Virol. 77*, 7856–7862.
49. Stiasny, K., and Heinz, F. X. (2006) Flavivirus membrane fusion. *J. Gen. Virol. 87*, 2755–2766.
50. Struck, D. K., Hoekstra, D., and Pagano, R. E. (1981) Use of resonance energy transfer to monitor membrane fusion. *Biochemistry 20*, 4093–4099.
51. Scott, W. R. P., Hunenberger, P. H., Tironi, I. G., Mark, A. E., Billeter, S. R., Fennen, J., Torda, A. E., Huber, T., Kruger, P., and van Gunsteren, W. F. (1999) The GROMOS biomolecular simulation program package. *J. Phys. Chem. A 103*, 3596–3607.
52. van Gunsteren, W. F., Billeter, S. R., Eising, A. A., Huenenberger, P. H., Krueger, P., Mark, A. E., Scott, W. R. P., and Tironi, I. G. (1996) Biomolecular Simulation: The GROMOS96 Manual and User Guide, VdF, Hochschulverlag AG an der ETH Zurich BIOMOS b.v., Zurich and Groningen.
53. Hol, W. G., van Duijnen, P. T., and Berendsen, H. J. (1978) The alpha-helix dipole and the properties of proteins. *Nature 273*, 443–446.
54. Ryckaert, J. P., Ciccotti, G., and Berendsen, H. J. C. (1977) Numerical-integration of Cartesian equations of motion of a system with constraints—molecular-dynamics of N-alkanes. *J. Comput. Phys. 23*, 327–341.
55. Tironi, I. G., Sperb, R., Smith, P. E., and van Gunsteren, W. F. (1995) A generalized reaction field method for molecular-dynamics simulations. *J. Chem. Phys. 102*, 5451–5459.
56. Bressanelli, S., Stiasny, K., Allison, S. L., Stura, E. A., Duquerroy, S., Lescar, J., Heinz, F. X., and Rey, F. A. (2004) Structure of a flavivirus envelope glycoprotein in its low-pH-induced membrane fusion conformation. *EMBO J. 23*, 728–738.

57. Pettersen, E. F., Goddard, T. D., Huang, C. C., Couch, G. S., Greenblatt, D. M., Meng, E. C., and Ferrin, T. E. (2004) UCSF Chimera—a visualization system for exploratory research and analysis. *J. Comput. Chem. 25*, 1605–1612.
58. Roehrig, J. T., Johnson, A. J., Hunt, A. R., Bolin, R. A., and Chu, M. C. (1990) Antibodies to dengue 2 virus E-glycoprotein synthetic peptides identify antigenic conformation. *Virology 177*, 668–675.
59. Provencher, S. W., and Glockner, J. (1981) Estimation of globular protein secondary structure from circular dichroism. *Biochemistry 20*, 33–37.
60. Sreerama, N., and Woody, R. W. (2000) Estimation of protein secondary structure from circular dichroism spectra: comparison of CONTIN, SELCON, and CDSSTR methods with an expanded reference set. *Anal. Biochem. 287*, 252–260.
61. Han, X., Bushweller, J. H., Cafiso, D. S., and Tamm, L. K. (2001) Membrane structure and fusion-triggering conformational change of the fusion domain from influenza hemagglutinin. *Nat. Struct. Biol. 8*, 715–720.
62. Corver, J., Ortiz, A., Allison, S. L., Schalich, J., Heinz, F. X., and Wilschut, J. (2000) Membrane fusion activity of tick-borne encephalitis virus and recombinant subviral particles in a liposomal model system. *Virology 269*, 37–46.
63. Stamatotos, L., and Silvius, J. R. (1987) Effects of cholesterol on the divalent cation-mediated interactions of vesicles containing amino and choline phospholipids. *Biochim. Biophys. Acta 905*, 81–90.
64. Brock, T. G., Nagaprakash, K., Margolis, D. I., and Smolen, J. E. (1994) Modeling degranulation with liposomes: effect of lipid composition on membrane fusion. *J. Membr. Biol. 141*, 139–148.
65. Gibbons, D. L., Vaney, M. C., Roussel, A., Vigouroux, A., Reilly, B., Lepault, J., Kielian, M., and Rey, F. A. (2004) Conformational change and protein-protein interactions of the fusion protein of Semliki Forest virus. *Nature 427*, 320–325.
66. Smaby, J. M., Momsen, M. M., Brockman, H. L., and Brown, R. E. (1997) Phosphatidylcholine acyl unsaturation modulates the decrease in interfacial elasticity induced by cholesterol. *Biophys. J. 73*, 1492–1505.
67. Bloom, M., Evans, E., and Mouritsen, O. G. (1991) Physical properties of the fluid lipid-bilayer component of cell membranes: a perspective. *Q. Rev. Biophys. 24*, 293–397.
68. Li, X. M., Momsen, M. M., Smaby, J. M., Brockman, H. L., and Brown, R. E. (2001) Cholesterol decreases the interfacial elasticity and detergent solubility of sphingomyelins. *Biochemistry 40*, 5954–5963.
69. Silvius, J. R. (2003) Role of cholesterol in lipid raft formation: lessons from lipid model systems. *Biochim. Biophys. Acta 1610*, 174–183.
70. Binder, W. H., Barragan, V., and Menger, F. M. (2003) Domains and rafts in lipid membranes. *Angew. Chem., Int. Ed. Engl. 42*, 5802–5827.
71. Simons, K., and Vaz, W. L. (2004) Model systems, lipid rafts, and cell membranes. *Annu. Rev. Biophys. Biomol. Struct. 33*, 269–295.
72. Han, X., and Tamm, L. K. (2000) A host-guest system to study structure-function relationships of membrane fusion peptides. *Proc. Natl. Acad. Sci. U.S.A. 97*, 13097–13102.
73. Han, X., and Tamm, L. K. (2000) pH-dependent self-association of influenza hemagglutinin fusion peptides in lipid bilayers. *J. Mol. Biol. 304*, 953–965.
74. Gasteiger, E., Gattiker, A., Hoogland, C., Ivanyi, I., Appel, R. D., and Bairoch, A. (2003) ExPASy: The proteomics server for in-depth protein knowledge and analysis. *Nucleic Acids Res. 31*, 3784–3788.
75. Miyauchi, K., Kim, Y., Latinovic, O., Morozov, V., and Melikyan, G. B. (2009) HIV enters cells via endocytosis and dynamin-dependent fusion with endosomes. *Cell, 137*, 433–444.